Palaeogeography, Palaeoclimatology, Palaeoecology (Global and Planetary Change Section), 89 (1990): 65–79
Elsevier Science Publishers B.V., Amsterdam

Variability of trace-metal fluxes through the Strait of Gibraltar

Alexander van Geen[1] and Edward Boyle

Department of Earth, Atmospheric and Planetary Sciences, Massachusetts Institute of Technology, Cambridge, MA 02139, U.S.A

(Received April 15, 1989; revised and accepted November 12, 1989)

ABSTRACT

Van Geen, A. and Boyle, A., 190. Variability of trace-metal fluxes through the Strait of Gibraltar. In: L.D. Labeyrie and C. Jeandel (Editors), Geochemical Variability in the Oceans, Ice and Sediments. Palaeogeogr., Palaeoclimatol., Palaeoecol. (Global Planet. Change Sect.), 89: 65–79..

Three water masses originating in the Atlantic and entering the Alboran Sea through the Strait of Gibraltar have recently been identified on the basis of salinity and Cu, Ni, Cd and Zn concentrations. The endmembers are (1) Atlantic surface water, (2) North Atlantic Central Water and (3) Spanish shelf water. Spanish shelf water is of particular relevance to the trace-metal composition of the inflow to the Mediterranean Sea because this water mass is highly enriched in Cu, Cd and Zn relative to Atlantic surface water.

Here, a conservative mixing model is solved for the above Atlantic endmembers, (with the addition of (4) a Mediterranean deep-water endmember) by weighted least-squares and shown to be consistent with tracer data for 42 surface samples collected in April '86 within the Strait of Gibraltar. Sensitivity of the solution to errors in the data and the assumptions of the model are discussed in detail. Uncertainties in the proportions of metal-enriched Spanish shelf water and NACW are (at most) on the order of 6 and 16%, respectively, and often smaller depending on the composition of a given sample. The inversion shows that Spanish shelf water is present predominantly in the northern half of the Strait and contributes up to 55% to Alboran Sea surface samples.

Determining a representative composition of the inflow is complicated, however, by rapid change in the proportion of the three Atlantic endmembers present in the Strait of Gibraltar: entrainment of Spanish shelf water through the Strait roughly doubles between April 11 and 17. We show that the timing of collection of these samples minimizes a potential bias in endmember distributions simply due to variable tidal currents. The increase in entrainment of Spanish shelf water from neap tide to spring tide could, therefore, reflect a significant shift to the north of source waters to the Atlantic inflow over the course of a week. The data show that entrainment of Spanish shelf water is a significant source of the increased Cu, Cd and Zn concentrations observed in the Mediterranean relative to open Atlantic surface water, and this source may even account for the greater part of the Mediterranean enrichments.

Introduction

Three water masses west of the Strait of Gibraltar show sharp contrasts in trace-metal concentrations. Relative to metal-depleted Atlantic surface water (1), Spanish coastal water (2) is highly enriched in Cu, Cd and Zn. To a lesser extent, North Atlantic Central Water (3) is enriched in Ni and Cd (Van Geen et al., 1988; Van Geen, 1989). The first goal of this paper is to exploit these circumstances to determine the distribution of identifiable mixtures of these water masses (and Mediterranean deep water (4)), in surface waters from the Strait of Gibraltar collected between April 11 and 19, 1986. The second objective is to determine how variability in the distribution of Atlantic water masses in the Strait over the course of a week affects estimation of the long-term average metal composition of Atlantic flow into the Mediterranean

---

[1] Present address: Department of Civil Engineering, Stanford University, Stanford, CA 94305, U.S.A.

0921-8181/90/$03.50

Sea. The justification for examining the composition of the inflow in such detail is that a comparison with the composition of the Mediterranean outflow through the Strait of Gibraltar places constraints on metal inputs (natural or anthropogenic) *within* the Mediterranean basin (Spivack et al., 1983).

The composition of the water masses west of the Strait of Gibraltar was recently determined on the basis of surface samples and profiles collected in March, April and October 1986 (Van Geen, 1989). Coastal (dissolved) metal enrichments in the Gulf of Cadiz due to a shelf-specific process or due to simple upwelling of North Atlantic Central Water (NACW) were distinguished by comparing shelf-water metal-salinity relationships in surface waters with those determined for vertical profiles collected in June '82 and in April '86 (Boyle et al., 1985; Van Geen, 1989). The data show that only part of Ni and Cd enrichments over the Spanish shelf could be attributed to mixing with deeper water. For Cu and Zn, there is no ambiguity since levels in Spanish coastal water are more than an order of magnitude higher than in Atlantic subsurface water of the same salinity. Shallow metal profiles from the Gulf of Cadiz show elevated concentrations of Cu, Cd and Zn extending over the top 40 m of the water column, suggesting a strong shelf-specific enrichment process for these elements (Van Geen, 1989).

The regression model which is applied decomposes each sample into Atlantic surface water, Spanish shelf water, NACW and Mediterranean deep water by assuming conservative mixing of salinity and Cu, Ni, Cd and Zn in the Strait of Gibraltar. Sensitivity of results to errors in the data or the composition of the endmembers is discussed in detail. The main result (which is robust) is that entrainment of Spanish shelf water roughly doubled between April 12 and 16. This illustrates the problem of determining a representative composition for the Atlantic inflow since the same endmember also exerts the strongest control on metal concentrations. Despite this source of uncertainty, it remains clear that entrainment of Spanish shelf water could explain much of the difference in Cu, Cd and Zn concentrations between Mediterranean and Atlantic surface water.

Sampling and analysis

We present here new data for 42 closely spaced surface samples distributed along partly overlapping transects across the Strait of Gibraltar, including eastern and western approaches to the Strait. Samples were collected as part of the Gibraltar Experiment (Kinder and Bryden, 1987) on April 11, 12 and 16–19 from USNS Lynch with a contamination-free underway-pumping apparatus. Salinity and nutrients were determined using standard techniques (Guildline Autosal salinometer and colorimetry, respectively) described in Strickland and Parsons (1968). Trace-metal analyses on 30-ml samples followed a resin pre-concentration procedure which has been automated (Van Geen and Boyle, 1990). All samples concentrates were analysed by graphite-furnace atomic absorption spectroscopy (Perkin-Elmer Zeeman 5000 and HGA 500). One-sigma precision for this data set is 5% or 0.2 nM for Cu and Ni whichever is larger, 6% or 6 pM for Cd and 6% or 0.3 nM for Zn. Blank corrections average 0.1 nM, 0.05 nM, <1 pM and 0.3 nM for Cu, Ni, Cd and Zn, respectively.

The conservative mixing model

Even though non-conservative processes play a role in determining the composition of water masses west of the Strait, it turns out that systematic metal-salinity and metal-metal relationships allow us to describe vertical and lateral variations in composition in the Gulf of Cadiz as the result of conservative mixing (Van Geen, 1989). As indicated by endmember compositions in Table 1, Atlantic surface water is depleted in all trace metals. Given the continuum of linear salinity–trace-metal relationships over the shelf, Spanish shelf water is somewhat arbitrarily defined by a salinity of 36.0 ‰ and corresponding Cu, Ni, Cd and Zn concentrations. This composition corresponds to water found at the north-west entrance to the Strait. Mediterranean deep water, defined on the basis of a

TABLE 1

Model matrix A contains the composition of the 4 endmembers of the regression. The standard error column is a measure of the degree to which each tracer contributes to the best fit solution for each sample

	Atlantic surface	Spanish shelf	NACW	Mediter. deep	Standard error
Salinity (‰)	36.30	36.00	35.70	38.45	0.1
Cu (nM)	1.0	6.6	1.3	1.9	0.33
Ni (nM)	2.2	3.4	2.6	4.6	0.33
Cd (pM)	30	190	135	77	10
Zn (nM)	0.8	21.0	1.5	4.8	1.0
Closure	1	1	1	1	0.001

profile collected in June '82 (Boyle et al., 1985) is added to the list of endmembers in order to describe stations in the Western Alboran Sea where this water mass outcrops at the surface. Endmember definitions have been revised relative to earlier work (Van Geen et al., 1988) based on a more extensive data set (Van Geen, 1989). The main differences are that Cu and Cd concentrations were decreased relative to Zn by 39 and 27%, respectively, for the definition of "100 %" Spanish shelf water, and that the Cd concentration in Atlantic surface water was increased from 20 to 30 pM. Nutrients and temperature cannot be used to determine endmember contributions in this situation since these tracers are highly non-conservative in surface water.

Assuming conservative mixing of salinity and trace metals, each surface sample in the Strait of Gibraltar (locations in Fig. 1; tracer data in Appendix) can be described as a linear combination of four distinct endmembers. In this expression, the weight of an endmember is the fraction of the total sample contributed by each source. In matrix notation, this relationship is expressed as:

$$A \cdot f = d \qquad (1)$$

where A is the $(6*4)$ model matrix whose top five rows contain the tracer composition of each endmember (= Table 1), $(6*1)$ vector d contains the composition of a specific sample and f is a $(4*1)$ vector whose four elements are the fractions of each contributing source which we want to estimate (Mackas et al., 1987). The fractions can not be negative and must sum to unity: a final line of factors equal to one added to the model matrix and to each column-data vector expresses this additional closure condition. The system is over-determined since there are 4 unknowns (the endmember fractions) and 6 linear equations (one for each tracer + the closure condition).

The solution need not match the data perfectly due to analytical errors and "real-world" deviations from the model. For each tracer, a residual is defined as the difference between observed and model-predicted data. Assuming the data follow Gaussian statistics, the best fit to each set of equations corresponding to a sample is obtained by minimizing the sum of the squared residuals (i.e., the L_2 norm, Menke, 1984). However, residuals must first be normalized with respect to each other by giving proper

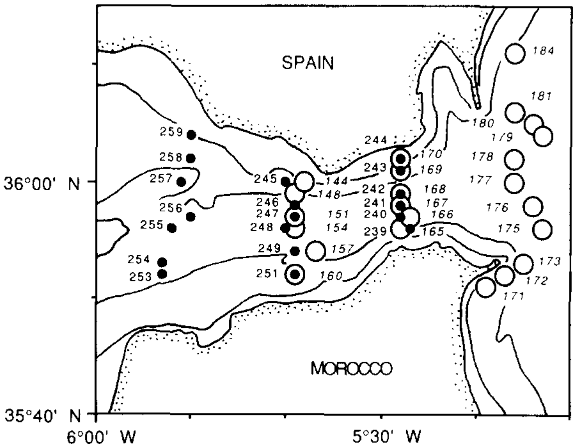

Fig. 1. Sample locations in the Strait of Gibraltar. Open circles correspond to samples collected April 11–12 (italics), filled dots to April 16–19. Isobaths at 50- and 200-m depth.

TABLE 2

Variance normalized model matrix $A_w = W \cdot A$. Weight matrix W is diagonal and composed of the inverses of the standard errors listed in Table 1

	Atlantic surface	Spanish shelf	NACW	Mediter. deep	Standard error
Salinity (%)	363	360	357	384.5	1
Cu (nM)	3.0	19.8	3.9	5.7	1
Ni (nM)	6.6	10.2	7.8	13.8	1
Cd (pM)	3	19	13.5	7.7	1
Zn (nM)	0.8	21	1.5	4.8	1
Closure	1000	1000	1000	1000	1

weights to each tracer equation. This is achieved by dividing all tracer values by their respective estimated standard errors which are also listed in Table 1. Error estimates are greater than (salinity) or comparable to (trace metals) analytical errors and represent the degree to which the model is required to fit the data for a given tracer. If W is a diagonal matrix composed of the inverse of estimated uncertainties for each tracer, the weighted model matrix becomes $A_w = W.A$ (Table 2). Similarly, tracer data at each station are converted to $d_w = W.d$. By this transformation, the variance of each tracer datum is, by definition, equal to one. Assuming errors in the data are uncorrelated (not necessarily true for "real-world" errors), off-diagonal elements of the data covariance matrix are set to zero. The closure condition is given a high weight of 1000, i.e., an error of 0.001, and forces the model parameters to add up to 1 within 0.1% for all samples. In contrast to the tracer equations, there is no justification for leaving any "slack" to the closure condition.

The least-squares solution to equation (1) for each surface sample is:

$$f = \left(A_w^t \cdot A_w\right)^{-1} \cdot A_w^t \cdot d_w. \tag{2}$$

Taking the additional inequality constraints into account, an iterative solution is found using the Kuhn-Tucker theorem (Menke, 1984). By this procedure, if the unconstrained best fit requires one of the endmember fractions to become negative, the solution becomes the next best fit with that fraction set to zero. This simple program was applied to each sample on a Tektronix 4052 computer. Matrix inverses are calculated by a supplied subroutine based on Gauss-Jordan triangularization. Before discussing in detail the distribution of the four endmembers in the Strait of Gibraltar and the Alboran Sea, the uncertainty in these solutions must be estimated.

How robust are the solutions?

Since both the model matrix A and the data d were premultiplied by the weight matrix W in the expression of the generalized inverse, the data covariance matrix becomes the identity matrix. How errors in the data are amplified as uncertainty in the model parameters can be

TABLE 3

Model parameter covariance matrix cov f, calculated from eqn. (3) in text. In parentheses under diagonal terms are square roots of the variances, and under off-diagonal terms the correlation coefficients

	Atlantic Surface	Spanish shelf	NACW	Mediter. deep
Atlantic Surface	0.0134 (12%)	0.0023 (+0.46)	−0.0117 (−0.90)	−0.0040 (−0.69)
Spanish shelf		0.0019 (4.4%)	−0.0033 (−0.67)	−0.0010 (−0.46)
NACW			0.0126 (11%)	0.0024 (+0.43)
Mediterranean deep				0.0025 (5.0%)

estimated from the unit covariance matrix of the model parameters:

$$\text{cov } f = \left(A_{\mathrm{w}}^{t} \cdot A_{\mathrm{w}}\right)^{-1} \tag{3}$$

Diagonal elements of cov f (see Table 3) are the variances of the model parameters. The uncertainty in each model parameter is estimated from the square root of the variance: 12% for Atlantic surface water, 4% for Spanish shelf water, 11% for NACW and 5% for Mediterranean deep water. These estimates depend on the structure of the model matrix and not on the composition of a specific sample. Non-zero off-diagonal terms of the covariance matrix indicate that the model parameters are not mutually independent. Atlantic surface water and NACW, for instance, are highly anti-correlated ($r = -0.90$).

The dynamic range separating endmembers for each tracer (A_{w}) is compared on a variance-normalized scale in Figure 2. The greater the range for a given tracer, the more useful it will be in resolving endmember contributions. Salinity dominates the estimate for the fraction of deep Mediterranean water, Zn and Cu dominate the estimate for the shelf endmember fraction, and Cd best resolves the deep Atlantic contribution after correction for Cd of shelf origin.

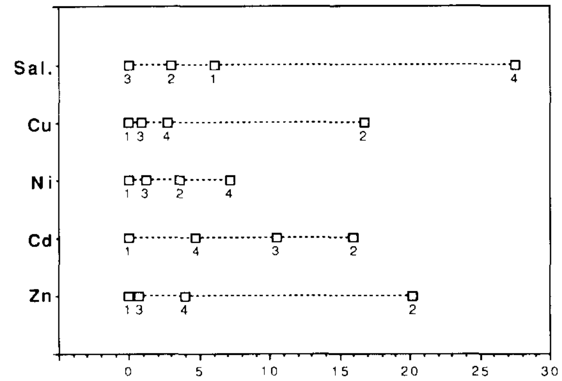

Fig. 2. Range of tracer composition of endmembers for normalized model matrix (Table 2). Value of endmember with lowest concentration was subtracted for each tracer. Indices correspond to (1) Atlantic surface water, (2) Spanish shelf water, (3) NACW, (4) Mediterranean deep water.

TABLE 4

Sensitivity of uncertainty in each endmember contribution (%) to disregarding each tracer in turn. Standard errors calculated from eqn. (3)

	Atlantic Surface	Spanish shelf	NACW	Mediter. deep
All 5 tracers				
+ closure	12	4	11	5
no salinity	14	5	12	16
no Cu	12	6	12	5
no Ni	12	4	11	5
no Cd	43	5	38	10
no Zn	12	7	13	5
All tracers				
No Med. water	8	4	10	–

The contribution of each tracer to the solution can be illustrated quantitatively be removing the constraint imposed by each tracer in turn. Standard errors for each model parameter are calculated from the modified covariance matrix (Table 4). This procedure quantifies the role of each tracer in determining the solution which was discussed qualitatively earlier. Without the salinity constraint, uncertainty in the Mediterranean contribution increases by a factor of three to 16%. Estimates of Atlantic surface and NACW contributions are strongly dependent on the Cd constraint: uncertainties increase to 43 and 38%, respectively, when neglecting this tracer. The contribution of the final endmember, Spanish shelf water, is better constrained than other members. Removal of either Cu or Zn does not significantly affect the variance of the solution. This indicates that, of these two tracers, one is redundant because of strong Cu and Zn enrichments in the same endmember.

The model parameter covariance matrix can be decomposed in greater detail by calculating the redistribution of endmember fractions due to a one standard error unit change in each tracer datum. The following expression is derived from equation (2):

$$\frac{\partial f}{\partial d} = A \cdot \left(A_t \cdot A\right)^{-1} \tag{4}$$

(subscript w becomes implicit)

Table 5 contains this (6∗4) matrix (neglecting the closure condition) and lists individual changes in endmember fractions. Again, the

TABLE 5

Endmember redistribution (in %) for one standard error unit change (Table 1) in each tracer datum: $\partial f/\partial d$ calculated from eqn. (4)

	Atlantic Surface	Spanish shelf	NACW	Mediterranean deep
Salinity	−1.8	−0.6	−1.3	3.8
Cu	1.7	2.7	−3.7	−0.7
Ni	−3.4	−0.4	2.0	1.8
Cd	−10.5	−0.8	9.2	2.1
Zn	2.2	3.3	−4.7	−0.8

Atlantic surface contribution is most sensitive to a change in Cd concentration of a sample (a 10% decrease for a +10 pM change in concentration), Spanish shelf water to Zn (+3.3% for +1 nM), NACW to Cd (+9% for +10 pM) and Mediterranean water to salinity (+4% for +0.1 ‰).

The dependence of the solution on the assumptions of the model is more difficult to determine than the sensitivity to the composition of a sample. Assumptions of the model are (1) the structure of the model matrix, i.e., the choice and composition of endmembers, and (2) conservative mixing. Assumption (2) of the mixing model implies the absence of significant external input or output mechanisms that could affect dissolved trace-metal concentrations in surface water. This is reasonable given the time scale of mixing in the Strait (on the order of days) and the oceanic geochemistry of trace metals (Bruland, 1983).

Returning to assumption (1), changes in endmember fractions caused by a variation in the model matrix *do* depend on the composition of a specific sample. This is in contrast to the uncertainty in the solution due to errors in the data which does not. Van Geen and Boyle (manuscript) recently estimated uncertainties for the composition of endmembers which are listed in Table 6. These estimates are based on the variability of composition of single endmembers where they can be observed: 40 offshore surface samples west of the Strait of Gibraltar for Atlantic surface water (Van Geen, 1989), and 11 samples of Mediterranean deep water (Boyle et al., 1985; Sherrell and Boyle, 1988). For endmembers which are not found in "pure" form, deviations from a simple mixing line with Atlantic surface water served to estimate uncertainties: 30 coastal water samples for Spanish shelf water, and a 12-point offshore profile for NACW. As shown in Table 6, the largest uncertainty resides in the composition of Spanish shelf water for all 5 tracers.

Since the propagation of errors due to uncertainty in tracer concentrations for the endmembers is cumbersome, changes in endmember composition were applied to two cases which are representative of the broad categories of samples found in the Strait: the first case contains 80% Atlantic surface water and 20% NACW, the second is a 50/50 mixture of Atlantic surface and Spanish shelf water. The test employed varies the composition of an endmember for each tracer in turn by the amount listed in Table 6 and then applies equation (2) to obtain the revised endmember composition. Deviations in endmember fractions from the initial mixture (80/20 or 50/50) for each of the five tracers were then squared and summed. In other words, each entry of Table 7 expresses the total variability in endmember proportion calculated from five separate inversions based on a slightly different model matrix.

In the first case (80/20), the effect of changes in the definition of Atlantic surface water on the solution is roughly 4 times larger than the effect of varying the definition of NACW. Contributions from either source of error, however, remain below that estimated from the data covariance matrix which reflects errors in the composi-

TABLE 6

Uncertainty in endmember tracer composition estimated from combination of natural and analytical variability

	Atlantic Surface	Spanish shelf	NACW	Mediterranean deep
Salinity (‰)	0.05	0.10	0.05	0.05
Cu (nM)	0.2	0.5	0.1	0.2
Ni (nM)	0.1	0.2	0.2	0.2
Cd (pM)	10	20	10	10
Zn (nM)	0.5	2	0.5	0.5

TABLE 7

Simulation results for two combinations of endmembers representative of the Strait of Gibraltar. Composition of contributing endmembers was changed by uncertainties listed in Table 6

	Atlantic Surface	Spanish shelf	NACW	Mediterranean deep
Change in composition of				
(1) Atlantic surface water	80 ± 7.8	0 ± 1.9	20 ± 7.1	0 ± 2.2
(2) NACW	80 ± 2.3	0 ± 0.4	20 ± 2.1	0 ± 0.6
Total error (with cov. matrix)	± 14%	± 5%	± 13%	± 5%
	Atlantic Surface	Spanish shelf	NACW	Mediterranean deep
Change in composition of				
(1) Atlantic surface water	50 ± 4.9	50 ± 1.2	0 ± 4.5	0 ± 1.4
(2) Spanish shelf water	50 ± 11.	50 ± 4.0	0 ± 11.	0 ± 3.0
Total error (with cov. matrix)	± 17%	± 6%	± 16%	± 6%

The first entry, for example, indicates that for a 80/20% mixture of Atlantic surface water and NACW (sample composition calculated from $d = A \cdot f$, the forward problem), (1) changing the tracer composition of Atlantic surface water by the uncertainty for each tracer in turn, (2) inverting 5 model matrices revised accordingly and calculating 5 new best-fit solutions for the sample whose *tracer* composition did not change (unlike its endmember composition), (3) summing squares of 5 corresponding deviations from 80% in Atlantic surface water proportion yields a value with a square root of 0.078 (7.8%). Note that endmembers not contributing to the initial mixture (in this case Spanish shelf water and Mediterranean water) were not constrained to remain positive in these simulations to avoid reducing the number of contributing endmembers in the inversion from 4 to 3, or 2.

tion of a sample. In principle, such a simulation should be applied individually to determine the total solution uncertainty for a specific sample. For our purpose, the sum of squared errors from the various sources for these two cases is sufficient. As shown in Table 7, the uncertainty in all endmember contributions for a sample containing mainly surface Atlantic water and NACW is increased by only 1 to 2% relative to the corresponding estimates from the covariance matrix alone. A 50/50 mixture of Atlantic surface water and Spanish shelf water, on the other hand, is considerably more sensitive to changes in endmember composition. Variations in the composition of Spanish shelf water have an effect twice that of changes in the composition of Atlantic surface water for this mixture. Adding estimates from the covariance matrix, total uncertainties in the solution become ±17%, ±6%, ±16% and ±6% for Atlantic surface water, Spanish shelf water, NACW and Mediterranean water, respectively. The last section of this paper shows that these ranges are, fortunately, smaller than actual variations in endmember distributions in the Strait of Gibraltar as a function of location and time.

Before discussing the distribution of endmembers in the Strait, consistency of the model with measured trace-metal concentrations is evaluated graphically by comparing measured and model-derived tracer data for the set of surface stations (Figure 3). How much weight a tracer datum carries in its own prediction in the least-square solution can be calculated from the $(6*6)$ data resolution matrix N (Menke, 1984) which relates observed and model-predicted data: $d^{\text{pre}} = N.d$. Predicted data, d^{pre}, are calculated by applying the forward problem to estimated model parameters: $d^{\text{pre}} = A \cdot f$. Substitution from (2) yields:

$$N = A \cdot (A^t \cdot A)^{-1} \cdot A^t \qquad (5)$$

Table 8 lists the data resolution matrix N calculated for this problem. Since predicted data are the product of observed data by the data resolution matrix, deviations from the identity matrix indicate that a predicted tracer value is a linear combination of its own and other ob-

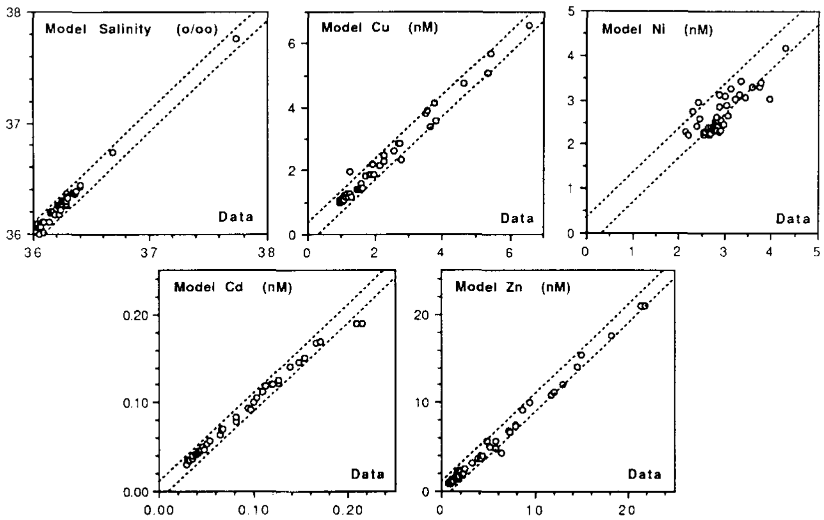

Fig. 3. Observed vs. model-predicted data from best fit. Diagonal bands indicate ± 1 standard error deviation (Table 1) from one to one correspondence.

served tracer values. Diagonal entries of the data resolution matrix are defined as the importance of the data in their own prediction. In decreasing order, the importance of the closure condition is 0.99, Cd: 0.94, salinity: 0.93, Zn: 0.60, Cu: 0.40, and Ni: 0.14. Off-diagonal entries are small for tracers with a high weight in their own prediction, such as Cd and salinity. Perhaps surprisingly, Zn and Cu have a low importance relative to their wide dynamic range. This is due to high co-linearity in the distributions of these two tracers which are dominated by the same endmember (Spanish shelf water, see also Fig. 2). Examination of the off-diagonal term relating these two tracers (0.49) indicates the importance of Cu and Zn in their own prediction has been replaced by a role in predicting each other.

In view of the structure of the data resolution matrix, it should be expected that tracers with a high importance, such as salinity and Cd, follow a one to one line in Figure 3 within the a priori error bands. This is because these tracers almost independently determine Mediterranean and NACW contributions, and therefore also control their own prediction. In contrast, tracers that are redundant (e.g., Ni vs. all other tracers, or Cu vs. Zn) and therefore do not control their own prediction, provide a verification of the conservative mixing hypothesis as well as the composition chosen for the endmembers. As it

TABLE 8

Data resolution matrix from eqn. (5)

	Salinity	Cu	Ni	Cd	Zn	1
Salinity	0.93	−0.02	0.24	−0.06	0.01	0.02
Cu		0.40	−0.00	0.01	0.49	0.01
Ni			0.14	0.23	0.00	−0.08
Cd				0.94	−0.01	0.02
Zn					0.60	−0.01
1						0.99

turns out, residuals are small also for the "weaker" tracers. In other words, the model is consistent with the data. It is worth noting that endmembers were chosen on the basis of actual profiles and surface samples from the Gulf of Cadiz and the Alboran Sea, i.e., independently of data from the Strait of Gibraltar.

Distribution of endmembers in the Strait of Gibraltar

The four-endmember regression model was applied to 42 surface samples from the Strait of Gibraltar (results in Appendix). The model excludes Mediterranean water from 18 of these samples. Where only three (Atlantic) endmembers are represented, the mixing model changes configuration. There are still 6 equations to be satisfied in the least-square sense but only three unknown model parameters. The new covariance matrix for this reduced system decreases the uncertainty due to errors in the data for Atlantic surface, Spanish shelf water, and NACW to 8%, 4%, and 10%, respectively (Table 4). Mediterranean deep-water contributions are greater or equal to 10% for only 6 samples (#171, 172, 179, 180, 181 and 184, see Fig. 1), all in the western Alboran Sea where upwelling occurs.

In April '86 (Fig. 4), surface waters of the Strait can be divided in two regions by a boundary roughly equidistant from each shore. The southern half is rather uniformly composed of 90–95% Atlantic surface water and 5–10% North Atlantic Central Water. To the north of this region, Spanish shelf water becomes the dominant contributor: up to 48% within the Strait on April 11–12, with sample #178 in the Alboran Sea containing as much as 55% Spanish shelf water. On April 16–19, the contribution of this endmember to surface water roughly doubles. At the same time, the maximum proportion of NACW in the Strait, 40% on April 11 (#144), decreases to less than 25% (#243) during the second sampling period. Considering the earlier estimates of the total uncertainty in Spanish shelf water and NACW (at most ±6% and ±16%, respectively), such variations in endmember distributions must be real since they are confirmed over several samples. It is worth noting that the two metal-enriched endmembers could not have been quantified in surface water by standard tracers since both Spanish shelf water and NACW are less saline than Atlantic surface water.

Transects at 5°40′ W and 5°30′ W on April 11–12 and 16–17 overlap and are the focus of the remaining discussion. Since tidal currents in the inflow layer oscillate by as much as ±200 cm s^{-1} around a long-term mean of roughly 40 cm s^{-1} to the east (Pettigrew and Needell, 1989), sample location and time of collection must first be related to the tidal cycle. Figure 5 shows that the transect at 5°40′ W started from the north on both April 11 and 16. In addition, sampling started on both occasions within one hour of Low Water at Gibraltar (LW) and ended at the time of the following High Water (HW). The implication is that samples from overlapping locations at 5°40′ W (Fig. 1) were taken several days apart at the same time relative to the phase of the diurnal cycle. The situation is similar for both sections at 5°30′ W even though samples were taken from south to north instead: both sections started at HW and reached the opposite shore at LW. Samples at the same location along 5°30′ W can, therefore, also be compared directly to each other without taking into account a bias in endmember distribution due to the phase of the tide. The implication of this timing is that changes in the distribution of endmembers between April 11–12 and April 16–17 do not simply reflect variability in tidal currents through the Strait of Gibraltar on the time scale of hours.

If diurnal tidal effects cannot explain variations in Spanish shelf water and NACW distributions between April 11 and 17 given the timing of sampling, another possibility is the spring-neap cycle. On April 11, the range between HW and LW was greatest (0.9 m), with a minimum in range following on April 18 (0.3 m). Gascard and Richez (1985) discuss in detail changes in the distribution of water masses in the Strait of Gibraltar between spring and neap tide based on measurements of classical tracers, temperature and salinity. During spring tide the

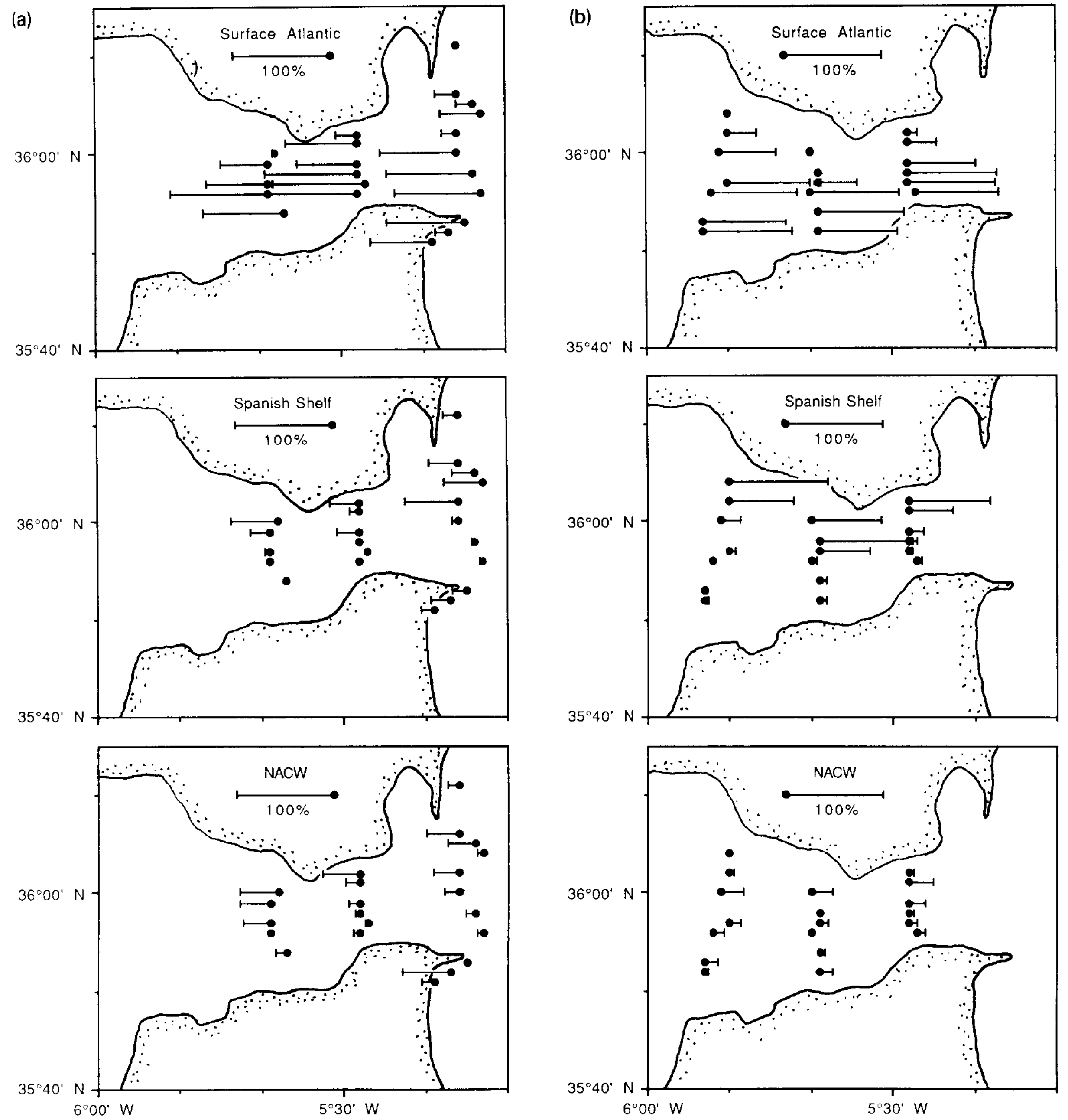

Fig. 4. Endmember distributions. a. On April 11–12. b. On April 16–19. Length of bar is proportional to contribution. Since only a few samples contain more than 10% Mediterranean water, all in the Alboran Sea, the distribution of this endmember is not shown. Sample #160 with high residual is not shown.

interface between in- and outflow (at 37.3‰ salinity) oscillates over a range of depths (≈ 80 m) roughly double of that during neap tide. Current oscillations are also stronger during spring tide, even though there is no significant difference in mean inflow velocity with neap tide. During neap tide, however, NACW does penetrate further east into the Strait as an identifiable subsurface low-salinity water mass. How do these observations compare to changes

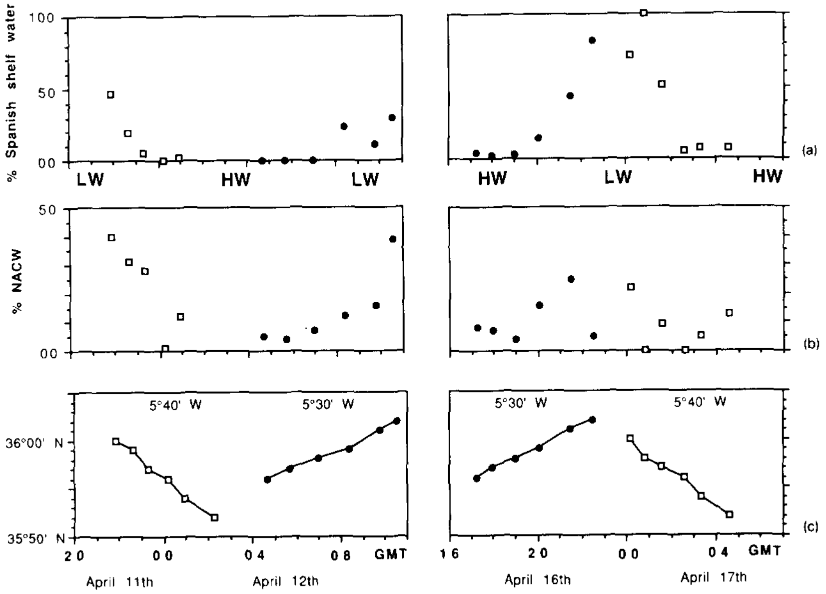

Fig. 5. a. Proportion of Spanish shelf water for transects at 5°40′ W and 5°30′ W on April 11–12 and 16–17 as a function of time relative to the tidal cycle at Gibraltar. (neap tide: April 11, spring tide: April 18). Note that first set of transects is centered at HW, the second set at LW.

b. Proportion of NACW for same transects.

c. Latitude of sample as a function of time to show streaming direction for each transect and help locate samples. Station locations in Fig. 1. The composition of sample 160 is not shown due to its large residual which suggests contamination.

in the distribution of Spanish shelf water and NACW inferred from our tracers? The simplest explanation compatible with the observed changes is that between spring tide (April 11) and neap tide (April 18), the source area of Atlantic water to the inflow shifted to the north, hereby entraining a greater proportion of Spanish shelf water at the expense of NACW. Evidently, greater subsurface penetration of NACW in the Strait of Gibraltar at neap tide is not traceable in surface water. The link between these results and the physical processes controlling the composition of the Atlantic inflow may be worth further study.

A rough estimate of the integrated change in composition of the inflow between April 12 and 17 can be obtained by averaging the contribution of Atlantic endmembers across the section at 5°30′ W. This approach does not present a problem regarding the proportion of entrained Spanish shelf water since CTD data of Bray (1986) obtained at the time of chemical sampling show a well-mixed surface layer in the northern portion of the Strait where this endmember dominates. The situation is less favorable in the case of NACW, particularly in the center and southern portion of the Strait. The same set of CTD casts indicates that at the 5°40′ W section, below a 50-m-thick surface mixed layer, the inflow is not homogeneous down to the interface with the saline outflow which is 100 m deeper (Sta. GB1131, GB 1198). Intrusion of NACW causes a salinity minimum at approximately 90-m depth. At 5°30′ W, the interface becomes shallower and the surface layer is vertically homogeneous on April 12, but not on April 17 when a salinity minimum is visible again. This concurs with the observation of Gascard and Richez (1985) discussed earlier regarding the penetration of NACW. One implication is that surface samples may underestimate the proportion of NACW entering the Alboran Sea during neap tide. The main problem with this estimation of the composition of the inflow, however, is that the current across a section of the Strait is not homogeneous and varies with time. If veloci-

TABLE 9

Estimate of composition of the Atlantic inflow at 5°30′ W calculated by averaging contributions of Atlantic endmembers to surface samples of the Strait of Gibraltar. Excluding small contributions of Mediterranean water yields, respectively, for Atlantic surface water, Spanish shelf water and NACW: 74.2, 11.3, 14.5% on April 12, 63.8, 25.4, 10.8% on April 16.

	April 12	April 16
Salinity (‰)	36.18	36.09
Cu (n*M*)	1.7	2.4
Ni (n*M*)	2.4	2.5
Cd (p(*M*))	63	82
Zn(n(*M*))	3.2	6.0

ties were higher in the northern part of the Strait, for instance, the proportion of Spanish shelf water entering the Mediterranean (and hence the flux of Cu, Cd and Zn) would be underestimated.

Despite these limitations, endmember averaging across the Strait at 5°30′ W for both April 12 and 16 and translation into tracer concentrations illustrates a simple point (Table 9). The range in Cu, Cd and Zn concentrations (1.6–2.2 n*M*, 59–79 p*M* and 3.0–5.8 n*M*, respectively) between the two sampling times is mostly due to the 11–25% variation in average Spanish shelf-water entrainment. It is worth noting also that Cu, Cd and Zn concentrations of the Mediterranean outflow (Table 1) are well within the range of variability in the composition of the inflow on the time scale of days which is estimated here. Ni concentrations in the outflow, on the other hand, are clearly elevated relative to the composition of the inflow. The uncertainty in the mean inflow concentration of this element is also lower than for other trace metals since Ni is not significantly enriched in Spanish shelf water.

Conclusion

Distributions of dissolved constituents Cu, Ni, Cd, Zn and salinity in the Strait of Gibraltar are consistent with conservative mixing of water masses contributing to the Atlantic inflow. These three water masses, (1) Atlantic surface water, (2) Spanish shelf water and (3) NACW, are also traceable in the western Alboran Sea. In the Alboran Sea, Mediterranean deep water must be added to the set of contributing endmembers.

A detailed error analysis and sensitivity study shows that the contribution of metal-enriched endmembers, Spanish shelf water and NACW are constrained (at worst) to ±6 and ±16% which compares favourably with variability in the Strait of Gibraltar ranging from 0% to 100% and 50%, respectively. While the mixing model is not strictly needed to determine the composition of the inflow, its successful application does bring forth systematic patterns in the distribution of trace metals, in particular, the strong presence of Spanish shelf water in the northern Strait of Gibraltar. The data suggest a significant shift to the north of Atlantic source waters to the inflow between spring tide and neap tide.

We have also shown that the main source of uncertainty in determining the mean composition of the inflow in this region is due to spatial and temporal variability of entrainment of Spanish shelf water. Based on samples taken one week apart in April '86, short-term variations in the composition of the inflow straddle the composition of the Mediterranean outflow. Such variability, combined with changes in the current pattern caused by the tidal cycle on even shorter time scales (hours), illustrates the difficulty in obtaining a representative composition of the inflow which can be compared to that of the outflow.

Surface samples from the Alboran Sea taken previously in June '82 (Van Geen et al., 1988) and later in October '86 (Van Geen, 1989) also show significant variations in the contribution of Spanish shelf water in the Alboran Sea. Such variability may be related to seasonal changes in the structure of the inflow discussed by Bormans et al. (1986) and compounds the problem of determining a representative inflow composition. Comparison of the composition of surface water in the Alboran Sea between June '82, April '86 and October '86 does suggest, however, that despite high frequency modulation in inflow composition (discussed in the present paper), Spanish shelf water remains a significant contributor over time scales of months to years.

From the range of metal inflow concentrations relative to the composition of the outflow, it appears that internal sources within the Mediterranean basin must be the major net contributors to the water column only for Ni; it is possible that for Cu, Zn, and Cd, the inflow provides most of the net flux into the Mediterranean. Such results place strong constraints on the relative magnitude of sources (rivers and aerosols) and sinks (scavenging of Cu, Ni, Cd and Zn) in the Mediterranean Sea (Van Geen, 1989).

Over even longer time scales, climate change may have affected source waters for the inflow and therefore the composition of the Mediterranean. Lowering of sea level during glacial time would have exposed the Atlantic Spanish shelf and limited processes which give rise today to very high dissolved metal concentrations in that region. Given the short residence time of water in the Mediterranean relative to the inflow (100 years), such a signal could be looked for in both planktonic and benthic foraminifera of the Mediterranean if shells of these organisms reflect ambient metal concentrations (Boyle, 1981).

Acknowledgements

Space and time were generously provided during the Gibraltar Experiment by Dr. T. Kinder and Dr. N. Bray on board USNS Lynch. M. Benno Blumenthal is thanked for very informative discussions on the regression model. J.F. Minster and an anonymous reviewer suggested significant improvements to the manuscript.

References

Bormans, M., Garrett, C. and Thompson, K., 1986. Seasonal variability of the surface inflow through the Strait of Gibraltar. Oceanol. Acta, 9(4): 403–414.

Boyle, E.A., 1981. Cadmium, zinc, copper, and barium in Foramimifera tests. Earth Planet. Sci. Lett., 53: 11–35.

Boyle, E.A., Chapnick, S.D., Bai, X.X. and Spivack, A.J., 1985. Trace metal enrichments in the Mediterranean Sea. Earth Planet. Sci. Lett., 74: 405–419.

Bray, N., 1986. Gibraltar Experiment CTD data report, SIO Reference series #86-21, Scripps Institution of Oceanography.

Bruland, K.W., 1983, Trace elements in sea-water. In: Chemical Oceanography, v. 8, Academic Press, London.

Candela, J., Winant, C.D. and Bryden, H.L., 1989, Meteorologically forced subinertial flows through the Strait of Gibraltar, J. Geophys. Res., 94: 12667–12679.

Gascard, J.C. and Richez, C., 1985. Water masses and circulation in the Western Alboran Sea and in the Strait of Gibraltar, Prog. Oceanogr., 15: 157–216.

Kinder, T.H. and Bryden, H.L., 1987. The 1985-86 Gibraltar Experiment: Data collection and preliminary results. EOS, Trans., Am. Geophys. Union, 68: 786–787, 793–795.

Mackas, D.L., Denman, K.L. and Bennett, A.F., 1987. Least squares multiple tracer analysis of water mass composition. J. Geophys. Res., 92: 2907–2918.

Menke, W., 1984. Geophysical data analysis-Discrete inverse theory, Academic Press, Orlando, CA.

Pettigrew, N.R. and Needell, G.J., 1989. Flow structure and variability in the Tarifa Narrows section of the Strait of Gibraltar, In: J.L. Almazan, H. Bryden, T. Kinder and G. Parilla (Editors), Seminario sobre la oceanografia fisica del Estrecho de Gibraltar. SECEG, Madrid.

Sherrell, R.M. and Boyle, E.A., 1988. Zinc, chromium, vanadium and iron in the Mediterranean Sea. Deep-Sea Res., 35: 1319–1334.

Spivack, A.J., Huested, S.S. and Boyle, E.A., 1983. Copper, Nickel and Cd in surface waters of the Mediterranean, In: C.S. Wong, E. Goldberg, K. Bruland and E. Boyle (Editors), Trace Metals in Seawater. Plenum Press, New York, NY, pp. 505–512.

Strickland, J.D.H. and Parsons, T.R., 1968. A practical handbook of seawater analysis, Fisheries Research Board of Canada.

Van Geen, A. and Boyle, E.A., 1990, Automated preconcentration of trace metals from seawater and freshwater. Anal. Chem., 62: 1705–1709.

Van Geen, A., Rosener, P. and Boyle, E., 1988. Entrainment of trace metal-enriched Atlantic shelf-water in the inflow to the Mediterranean Sea. Nature, 331: 423–426.

Van Geen, A., 1989. Trace Metal Sources for the Atlantic Inflow to the Mediterranean Sea. Ph.D. Thesis. MIT/WHOI, WHOI-89-17.

APPENDIX 1A

Time of collection, location and composition of 42 samples within the Strait of Gibraltar, including western and eastern approaches to the Strait. Silicate and phosphate concentrations in μM, Cu, Ni and Zn in nM, Cd in pM. End-member fractions obtained by linear regression discussed in text. Five tracers were used for inversion of each sample composition. Residual column lists sum of squared residuals in variance normalized standard error units (eg. for salinity, one unit corresponds to 0.1‰). A sample whose composition agrees within one standard error with model-derived concentrations for all five tracers has a total residual ≤ 5. In this data set, only 3 samples residuals > 5: #160 (12.5), 170 (6.2) and 259 (5.8).

Station	Date	GMT	Latitude		Longitude		Silicate	Phosphate
144	April 11th	21:52	36	0	-5	38	1.5	0.20
148		22:36	35	59	-5	39	0.8	0.08
151		23:18	35	57	-5	39	1.0	0.10
154	April 12th	00:12	35	56	-5	39	0.9	0.19
157		00:55	35	54	-5	37	2.7	0.10
160		02:16	35	52	-5	39	1.4	0.16
165		04:40	35	56	-5	28	1.0	0.13
166		05:43	35	57	-5	27	1.4	0.13
167		07:00	35	58	-5	28	1.6	0.18
168		08:23	35	59	-5	28	1.7	0.14
169		09:46	36	1	-5	28	1.6	0.17
170		10:32	36	2	-5	28	1.5	0.19
171		12:40	35	51	-5	19	1.2	0.09
172		13:00	35	52	-5	17	1.1	0.08
173		13:33	35	53	-5	15	1.2	0.10
175		14:54	35	56	-5	13	1.2	0.12
176		16:00	35	58	-5	14	1.1	0.12
177		17:07	36	0	-5	16	1.3	0.12
178		18:04	36	2	-5	16	1.4	0.20
179		18:29	36	4	-5	13	2.1	0.19
180		19:36	36	5	-5	14	2.4	0.22
181		19:56	36	6	-5	16	3.2	0.22
184		22:04	36	11	-5	16	3.2	0.17
239	April 16th	17:18	35	56	-5	27	0.8	0.14
240		18:00	35	57	-5	28	0.9	0.13
241		19:00	35	58	-5	28		0.08
242		20:06	35	59	-5	28		0.09
243		21:28	36	1	-5	28		0.17
244		22:30	36	2	-5	28		0.23
245	April 17th	00:12	36	0	-5	40		0.38
246		00:50	35	58	-5	39		0.22
247		01:34	35	57	-5	39		0.10
248		02:35	35	56	-5	40		0.05
249		03:19	35	54	-5	39		0.12
251		04:36	35	52	-5	39		0.16
253	April 18th	22:15	35	52	-5	53		
254		22:35	35	53	-5	53		0.06
255		23:27	35	56	-5	52		0.20
256	April 19th	00:20	35	57	-5	50	0.8	0.24
257		02:00	36	0	-5	51	0.8	0.07
258		02:41	36	2	-5	50	1.3	0.20
259		03:22	36	4	-5	50	1.5	0.15

APPENDIX 1B

Station	Salinity	Cu	Ni	Cd	Zn	SurfAtl	Shelf	NACW	Medit.	Residual
144	36.131	3.3	2.7	150	11.4	0.04	0.47	0.40	0.09	2.0
148	36.091	1.8	2.7	91	5.5	0.47	0.19	0.31	0.03	1.5
151	36.161	1.4	2.8	64	2.0	0.63	0.05	0.28	0.04	3.0
154	36.285	0.9	2.1	29	0.8	0.99	0.00	0.01	0.00	0.0
157	36.285	1.2	2.0	47	1.0	0.83	0.02	0.12	0.02	0.5
160	36.282	1.2	2.2	95	6.1	0.43	0.15	0.33	0.09	9.7
165	36.253	0.9	2.5	31	0.9	0.94	0.00	0.05	0.01	2.1
166	36.251	0.9	2.5	30	1.0	0.95	0.00	0.04	0.01	2.2
167	36.267	0.9	2.4	35	0.8	0.91	0.00	0.07	0.02	1.1
168	36.231	2.1	2.3	79	5.6	0.62	0.23	0.12	0.03	0.1
169	36.181	1.5	2.3	63	3.2	0.73	0.11	0.16	0.00	0.0
170	36.215	2.5	2.3	124	7.6	0.22	0.30	0.39	0.09	3.2
171	36.409	1.7	2.9	66	4.0	0.62	0.13	0.13	0.12	1.7
172	36.354	2.6	3.1	117	4.6	0.13	0.19	0.49	0.20	3.1
173	36.356	1.7	2.6	52	4.2	0.79	0.15	0.00	0.06	0.9
175	36.299	1.1	2.5	40	1.8	0.88	0.04	0.06	0.03	0.7
176	36.218	1.2	2.5	42	1.6	0.87	0.04	0.09	0.01	1.0
177	36.193	1.4	2.6	53	2.4	0.77	0.07	0.14	0.02	1.8
178	36.063	3.5	2.8	144	12.7	0.15	0.54	0.27	0.04	1.8
179	36.400	3.4	3.2	100	8.5	0.42	0.39	0.06	0.13	2.5
180	36.693	2.4	3.5	106	7.0	0.17	0.23	0.28	0.31	2.2
181	36.284	2.6	3.7	110	7.6	0.21	0.29	0.33	0.17	8.9
184	37.742	2.1	4.0	97	7.1	0.01	0.14	0.12	0.73	0.8
239	36.282	1.0	2.6	42	2.2	0.84	0.04	0.08	0.04	2.4
240	36.283	1.0	2.4	39	1.6	0.88	0.02	0.07	0.03	0.9
241	36.280	1.0	2.7	35	1.7	0.91	0.03	0.04	0.03	2.6
242	36.143	1.6	2.7	65	4.0	0.69	0.14	0.16	0.01	2.3
243	36.051	3.5	2.7	124	9.2	0.30	0.44	0.25	0.02	0.8
244	36.060	5.0	3.4	163	17.8	0.09	0.82	0.05	0.03	2.0
245	36.061	5.0	2.9	167	14.6	0.02	0.71	0.22	0.04	1.0
246	36.054	6.1	3.6	204	20.9	0.00	1.00	0.00	0.00	5.1
247	36.038	3.3	2.9	116	11.8	0.40	0.51	0.09	0.00	2.0
248	36.347	1.1	2.5	35	2.2	0.91	0.05	0.00	0.04	1.5
249	36.245	1.5	2.5	43	1.7	0.87	0.07	0.05	0.01	1.9
251	36.167	1.5	2.4	50	1.7	0.81	0.07	0.13	0.00	1.4
253	36.298	1.1	2.6	34	1.6	0.91	0.03	0.02	0.03	2.4
254	36.214	1.0	2.6	41	1.1	0.84	0.01	0.13	0.02	2.5
255	36.234	0.9	2.8	38	0.7	0.87	0.00	0.11	0.02	3.9
256	36.153	1.4	2.7	45	1.7	0.83	0.06	0.11	0.00	4.0
257	36.074	2.0	2.6	80	4.9	0.58	0.20	0.22	0.00	0.9
258	36.029	4.3	3.0	135	14.1	0.29	0.66	0.05	0.00	0.7
259	36.086	6.1	3.1	211	21.3	0.00	1.00	0.00	0.00	7.4

Note added in proof

(Candela et al. (1989) find that 12% of the variance in transport through the Strait is modulated by the spring-neap cycle. Greater entrainment of Spanish shelf water on April 16–17 could therefore reflect the observed increase in exchange of waters between the Atlantic and the Mediterranean at neap tides.